ISSN 2176-5480

22nd International Congress of Mechanical Engineering (COBEM 2013)
November 3-7, 2013, Ribeirão Preto, SP, Brazil

NUMERICAL INVESTIGATION OF BONDED PANEL UNDER COMPRESSIVE LOADING

Andréa Izumi Fukue Massuda
Flávio Luiz de Silva Bussamra
Instituto Tecnológico de Aeronautica. Praça Marechal Eduardo Gomes, 50 - Vila das Acácias, S. J. Campos/SP
andreaif@yahoo.com.br', flaviobu@ita.br

Francisco Kioshi Arakaki
Embraer S.A. Av. dos Astronautas, 1270 - Putim, S.J. Campos/SP
francisco.arakaki@embraer.com.br

Eliseu Lucena Neto
Instituto Tecnológico de Aeronautica. Praça Marechal Eduardo Gomes, 50 - Vila das Acácias, S. J. Campos/SP
eliseu@ita.br

Abstract. *The objective of this study is to investigate a finite element model based on ABAQUS computer program to evaluate stresses in bonded reinforced panels subjected to compressive loads. It is intended to access not only the stress in the skin and stringers, but mainly to observe the behavior of the structural adhesive. The model proposed in this analysis was able to produce good results on the prediction of theoretical buckling load, compared with the finite element model (FEM). It was possible to evaluate the buckling load of the panel and stringers as well as the load of the initial degradation of the adhesive and its subsequent failure. Experimental tests are needed to check the tests results and theory. Furthermore, research should be conducted around the adhesive failure criteria.*

Keywords: *Bonding, Non-linear analysis, Adhesive, Buckling, Post-buckling*

1. INTRODUCTION

This study aims to make a numerical investigation of bonded panel under compressive loading combined with instability analysis (panel buckling). It will be performed buckling and post-buckling analysis of the panel, as well as, the determination of the failure load of the adhesive. At the end it will be possible to produce a diagram of load versus evolution of the failure mode (buckling, yielding, post buckling and collapse) of the panel.

Adherents were modeled as shell elements and the adhesive as a cohesive surface. A non-linear analysis is required for this evaluation so that the yield behavior at skin and stringers can be captured. Several factors must be considered in this analysis such as, failure mode of the adhesive, finite element model mesh refinement, load applied, boundary conditions, among others.

According to Dean and Crocker (2001), bonded joints may fail due to the initiation and/or crack growth (adhesive disbonding). Crack in the adhesive occurs because of the type of joint geometry, the type of adhesive, the applied load, the boundary conditions, etc. The crack in the adhesive joint will begin in the stress concentration region. The critical stress or deformation level should be determined in that region. It is known that the adhesives are not resistant to high normal stress components (peel), so it should be avoided the assembly work in this system.

Bonded joints subjected to compressive loads can experience buckling event. Buckling is a phenomenon that occurs in structures subjected to compressive loads. This is a structural instability, where the material has not fully reached its yield stress in the linear portion of the material. This collapse occurs in the direction of the axis of the smallest moment of inertia in the cross section. The critical buckling stress (F_{cr}) is not directly dependent of yield stress but the Young's modulus (E) of the material.

As studied by Megson (1999), a thin plate may buckle in different ways depending on its dimensions, applied loading and boundary conditions. When comparing buckling loads between beams and plates, in the case of the beams when it reaches its buckling load it can no longer resist to the axial loads and thus the critical load is the failure load of the structure (Rizzi, 2007). However, in the case of reinforced plates, after reaching the critical buckling load, the structure is still able to withstand increased compressive forces and will not fail until a load bigger than the critical load is reached. In other words, the critical load for buckling will not be the failure of the structure. One way to guarantee the maximum load plate is taking into account the post-buckling behavior.

To obtain the critical buckling load (P_{cr}) to plates is similar to the Euler's method made for beam structures. The load is dependent on the ratio between the width and the thickness plate. As smaller is the thickness, lower is the critical buckling load (Paulino, 2009).

This consideration is applicable to a perfectly flat plate simply supported with compressed edges (applied load q_y) and other edges free (Figure 1). In this analysis, the buckling loads of compression will be agreed with positive voltages and signal strength in order to facilitate the interpretation of the data.

ISSN 2176-5480

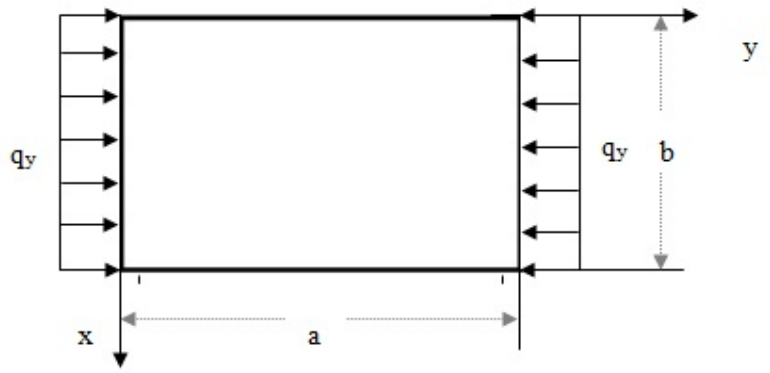

Figure 1. Buckling in Plates (Paulino, 2009)

The critical buckling stress is given by Eq. (1), as shown in Megson (1999):

$$F_{cr} = K_C \frac{E}{12(1-\nu^2)} \pi^2 \left(\frac{t_{panel}}{b_{panel}} \right)^2 \quad (1)$$

Where F_{cr} is the critical buckling stress in MPa, K_C is the buckling compression coefficient, E is the Young's modulus in MPa, ν is the Poisson coefficient, t_{panel} is the panel thickness in mm and b_{panel} is the panel width also in mm. In this case, K_c will be 6.98 extracted from literature.

With the cross-sectional area (A_s) it is obtained the buckling load F_{cr} multiplying by A_s, as shown in the Eq. (2):

$$P_{cr} = F_{cr} * A_s \quad (2)$$

The eigenvalue is a number commonly used to estimate the critical load of "stiffness" of the structures. It is a linear perturbation method and may be the first step of an analysis of a structure subjected to compressive loads. The linearized buckling, also known as eigenvalue buckling, applied to materials with linear constitutive relationship is based on obtaining the eigenvalues (Jacob, 2011). It is possible to obtain loads and buckling modes by solving an eigenvalue problem as shown in Eq. (3). Eigenvalues and eigenvectors are determined numerically using subspace iterations by the algorithm available in ABAQUS (Nascimento, 2010)

$$\left([K_0 + \lambda [\Delta K_G]] \right) \{\phi\} = \{0\} \quad (3)$$

Where: K_0 is the stiffness matrix, λ is the eigenvalue; ΔK_G is the geometric stiffness matrix and ϕ the eigenvectors.

After obtaining the eigenvalues, the compressive stress is expected to occur only in the elastic region of the material curve. The critical buckling load is solved by Eq. (4). The average buckling stress is calculated according to equation (5). The total load is the sum of the reaction forces (P_T) on the plate edges, due to prescribed displacement applied to the finite element model.

$$P_{cr} = \lambda * P_T \quad (4)$$

$$F_{cr} = \frac{P_{cr}}{A_s} \quad (5)$$

Where: F_{cr} is the critical buckling stress in MPa, P_{cr} is the critical buckling load in N, A_S is the total cross-sectional area in mm^2, P_T is the total applied load in N.

When evaluating the post-buckling behavior is noted that the collapse of a structure basically occurs in two ways (Camotim and Reis, 2000):

- By material rupture;
- By instability of structure.

ISSN 2176-5480

In the first way, the collapse occurs when the structure reaches the yield strength of the material and the second is due to the mechanism of structural instability. In some structures, the collapse may occur due to loss of stability with smaller stress levels to the strength of the material. For thin plates, the concept of geometric nonlinearities and imperfections should be taken into account. The introduction of geometric nonlinearities is very important to evaluate structures susceptible to buckling loads, because it shows a phenomenon that cannot be observed in linear analysis. There may be several configurations of equilibrium (stable and unstable) as well as maximum and minimum points along the nonlinear structure. Thin plates have the advantage to redistribute compressive axial loads efficiently in plane even after buckling (Castelani, 2012). The models studied here do not take into account geometric imperfections in the initial analysis.

2. MATERIALS AND METHODOLOGY

This section presents the mechanical properties of materials and the method of analysis used in this study. It required a model that takes geometric and material nonlinearities. Table 1 shows the mechanical properties of the materials used: Aluminum 2024-T3 for skin and Al 7075-T62 for stringers Table 2 shows the material data of the adhesive used.

Table 1. Mechanical Properties of Aluminum (MMPDS-03, 2006)

Material	E (MPa)	Poisson	F_{tu} (MPa)	F_{ty} (MPa)	F_{cy} (MPa)	ρ (t/mm^3)
Al 2024-T3	73774	0.33	434	290	269	2.768E-06
Al 7075-T62	71705	0.33	517	448	490	2.796E-06

Table 2. Elastic Properties of Adhesive (ABAQUS, 2010)

Material	E (MPa)	G_{13} (MPa)	G_{23} (MPa)	N_0 (MPa)	T_0 (MPa)	S_0 (MPa)	G_{1C} (N/mm)	G_{2C} (N/mm)	G_{3C} (N/mm)	η
ABAQUS (2010)	1E+06	1E+06	1E+06	61	68	68	0.075	0.547	0.547	1.45

The plastic behavior of a material is described when it exceeds the yield stress of the material in the stress-strain curve. The deformation of the material before reaching the yield point creates only elastic deformations, which are completely recovered if the applied load is removed. However, when the load applied creates a stress that exceeds the yield stress of the material, the occurrence of permanent deformation (plastic) begins. Deformations associated with these permanent deformations are called plastic deformation. Both deformation (elastic and plastic) are accumulated when the metal is deformed in the region of post-yielding (ABAQUS, 2010).

Eq. (6) e (7) relates nominal stress versus true stress as well as the relationship between true strain and plastic strain of material. Where: σ_{true} is the true stress in MPa, ε_{true} is the true strain, ε_p is the plastic strain and E is the Young's modulus in MPa. Figure 2 shows the true stress versus plastic strain curve for Al 2024-T3 and Al 7075-T62.

$$\sigma_{true} = \sigma_{nom}\,(1 + \varepsilon_{nom}) \tag{6}$$

$$\varepsilon_p = \varepsilon_{true} - \frac{\sigma_{true}}{E} \tag{7}$$

There are a lot of elements to modeling bonded joints with adhesives, interfaces assemblies with composite material among other situations where there is interest in verifying the integrity and strength of the bonded interfaces. For a better response of the post-processing of bonded joint it is required proper modeling which involves: choice of the element mesh, choice of appropriate cohesive interface (adhesive as cohesive surface), definition of materials' mechanical properties, definition of the behavior of degradation and failure of the adhesive, choice of the boundary conditions (herein referred to as BC), convergence analysis to determine the best number of elements, application of the load (in this case will be applied prescribed displacement in the structure in order to give the same displacement for all assembly), execution of static, buckling and post-buckling analyses and finally obtain and analyze the results. Mechanical properties such as stiffness and strength of the adhesive can be experimentally measured and used directly in modeling. In general, the adhesive material behaves better than the adjacent materials. The cohesive surface models the initiation of damage and degradation of the adhesive which will result in damage propagation leading to material failure.

ISSN 2176-5480

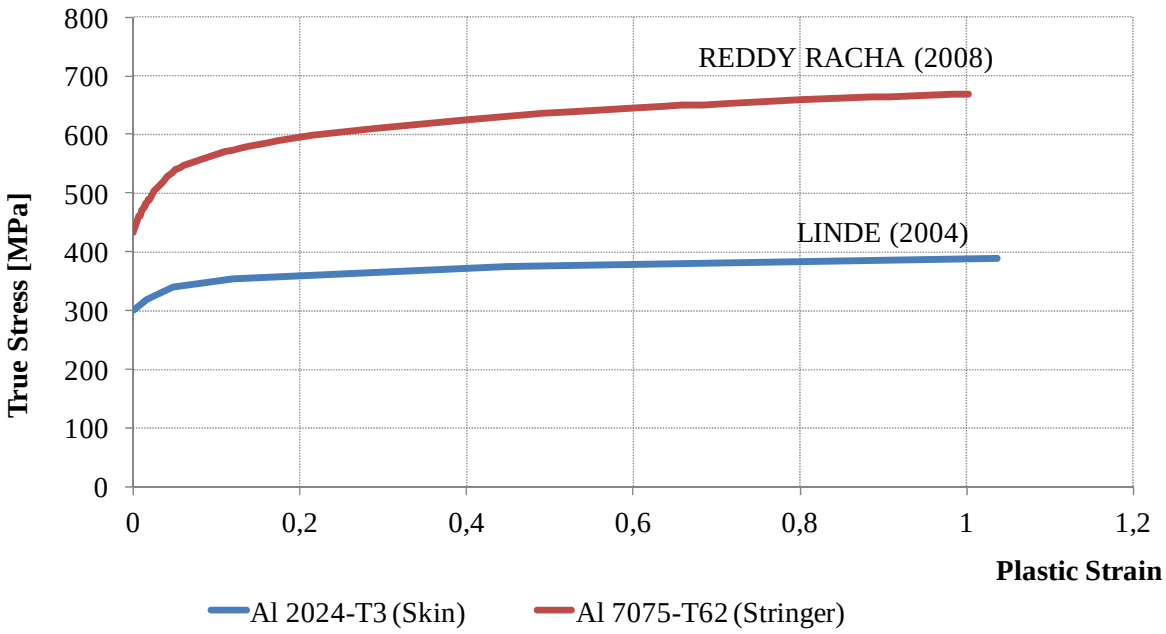

Figure 2. True Stress versus Plastic Strain

The modeling of the adhesive using *ABAQUS* (2010) involves choosing two pairs of surfaces that will be in contact with each other. This connection is given by the surface element's node. It is not necessary that the two meshes are coincident, the stiffest surface is the dependent one (slave) and it's also the most refined. The other surface will be the less refined (master).

Besides applying the contact technique, the adhesive in *ABAQUS* (2010) is based on the surface cohesive traction-separation behavior, and subject to the degradation and failure laws.

Modeling bonded interfaces often involve situations where the thickness of the adhesive material is so thin that in practice can be considered as zero. Cohesive surfaces should be used in areas where it is expected the development of cracks. However, there is no need to add the cracks to finite element model where they are to be initiated. Actually the exact location where the cracks will start, as well as the characteristics of the evolution of each crack are determined as part of the solution. The cracks and disbonding are restricted to propagate along the interface and not deviate to adjacent areas of the material (*ABAQUS*, 2010).

Surfaces based on cohesive behavior are used primarily when the thickness of the interface is significantly small. If the adhesive layer has finite thickness and macroscopic properties (such as stiffness and strength) of the adhesive are available, may be more appropriate to model the response using the conventional cohesive elements.

Cohesive zone is determined in terms of traction-separation. For each failure mode (mode I, II e III) is defined the degradation curve (T_0, N_0, S_0).

When one of the criteria reaches the value 1, begins the degradation of the adhesive evaluated by criterion *CSQUADSC*, continues the evolution of the damage and its subsequent failure is shown by criterion *CSDMG*.

Three cohesive parameters are used to define the cohesive zone. They are: the energy release rate G_c (needed to separate bonded surface), the maximum tension or cohesive strength of the interface (T_0, N_0, S_0) and the stiffness of the interface (K).

According to Ramamurthi (2012) when the tension reaches the value of tensile strength (T_0), damage (disbonding) begins. The displacement of the point is known as Initiation Displacement in the beginning of the damage (δ_0). After this point the delamination propagates. In other words, when damage reaches T_0, the degradation is complete. Then the adhesive begins to fail, the damage progresses (propagates) culminating in the total failure of the adhesive that occurs at a distance called the separation distance (δ_f). From this point is the total failure of the adhesive. The area under the curve is called G_c (Energy Release Rate).

Figure 3 shows the traction separation curve, where: K is the stiffness, δ_0 is the distance from the beginning of the separation, δ_f is the separation distance, T_0 is the cohesive strength in traction and G_c is the energy release rate in MPa. The interface between the skin and stringers is represented by the Interaction Properties which has the adhesive allowable.

ISSN 2176-5480

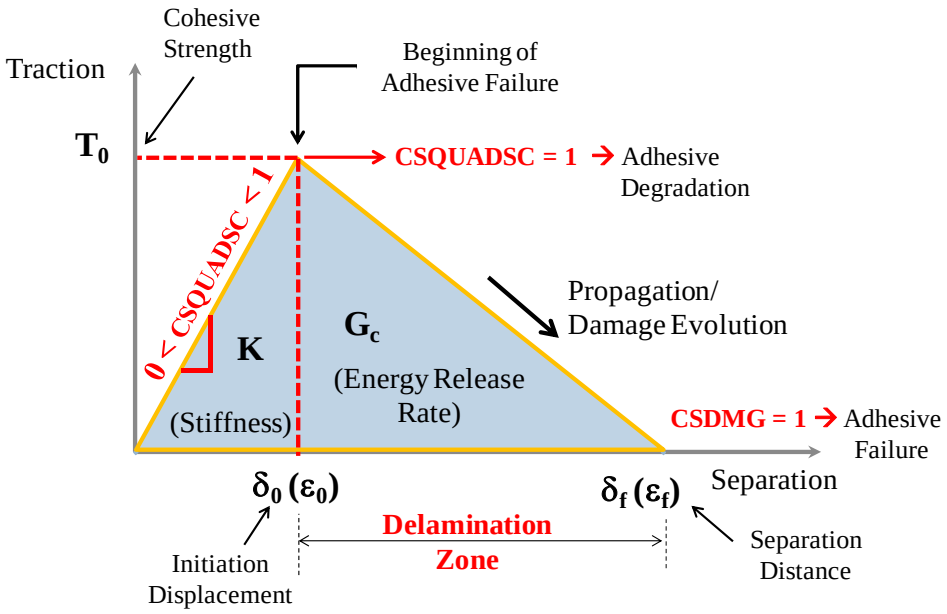

Figure 3. Cohesive Zone Model (GAVAZZI, 2012)

3. FINITE ELEMENT MODELS (FEM)

Figure 4 shows the element mesh of the assembly skin-stringer bonded with adhesive between their interfaces.

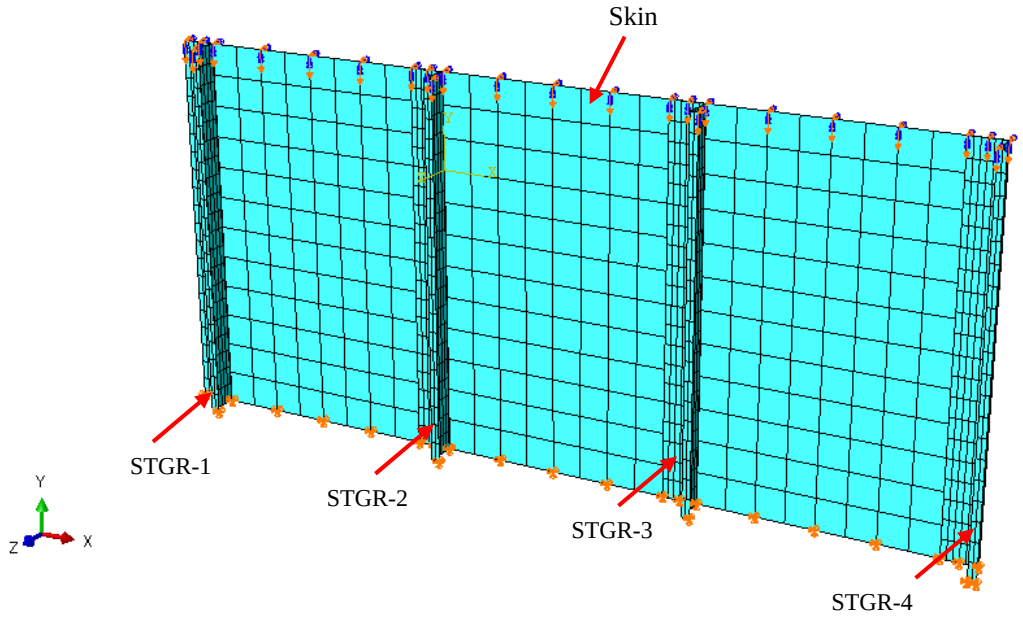

Figure 4. Model using ABAQUS (Finite Element Mesh)

These models are focused on structural analysis of a reinforced bonded panel subjected to compressive loads. This panel will be analyzed with the help of the computer program *ABAQUS* (2010, version 6.10), which is based on finite element method and follows the materials' properties laws through computational mechanics. With the displacements applied, will be evaluated the stresses and reaction forces at the panel edges. Furthermore, it will be possible to observe the degradation behavior of the adhesive and structural failure between the skin and the stringers. Adherents were modeled as shell elements because are simpler and easier to model, bring satisfactory results, besides saving computational time. The adhesive layer at the interface skin-stringer was modeled as cohesive surface and interaction properties between parts.

ISSN 2176-5480

The panel modeling consists on the application of boundary conditions on the top and bottom edges of it, the lateral edges are free. The loading is applied in the prescribed displacement form of-1mm in the axial direction of the stringers. Three variations of boundary conditions will be presented.

The panel comprises of an aluminum 2024-T3 1.016 mm skin thickness, reinforced with 4-stringers made of Al 7075-T62 aluminum (extruded) bonded with structural adhesive, as shown in Figure 5. Stringers are placed at constant distances from each other.

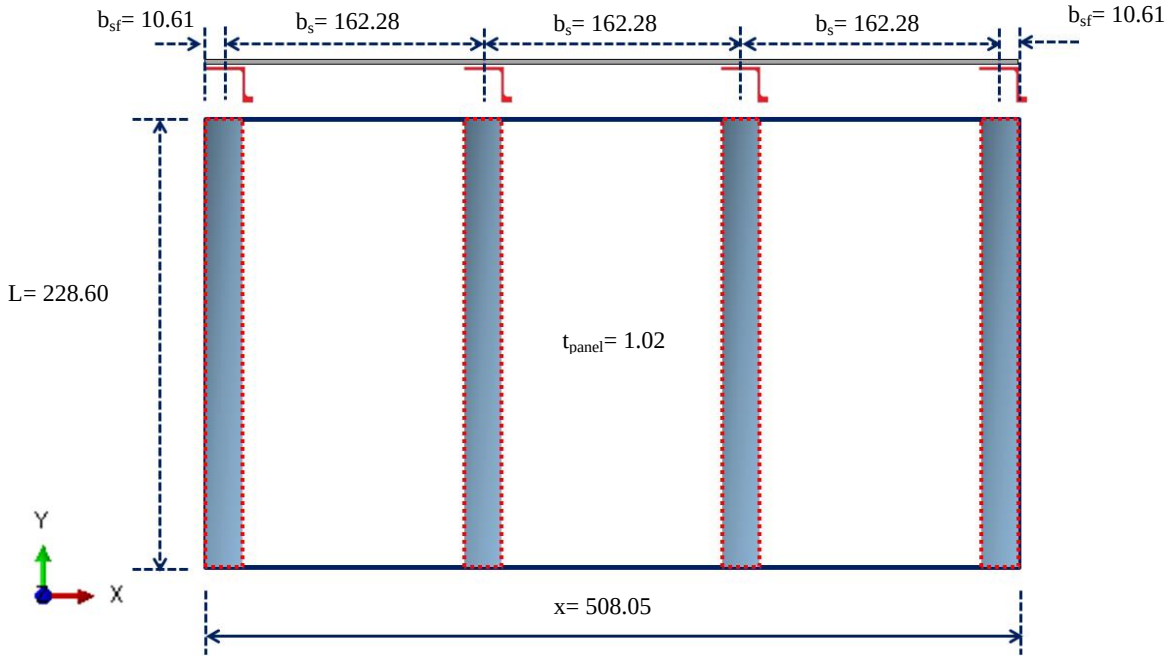

Figure 5. Reinforced Panel (measure in mm)

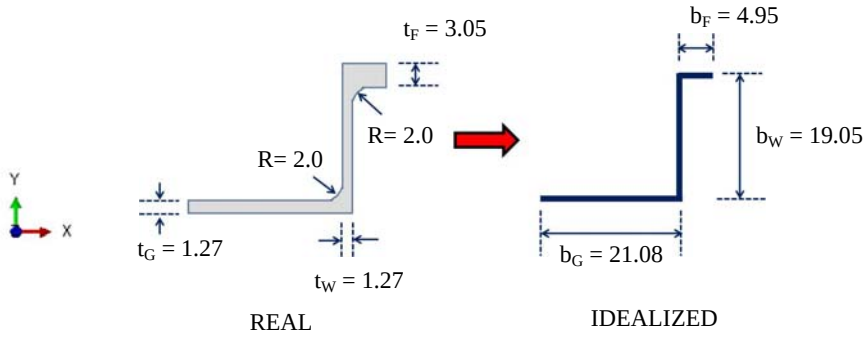

Figure 6. Stringer (measure in mm)

Several boundary conditions were investigated. The degrees of freedom of translational and rotational direction were convention as shown in Figure 7. It refers to global system model. Each degree of freedom (D.O.F.) is described below:

Table 3. Degree of Freedom (D.O.F.)

	D.O.F. 1	**D.O.F. 2**	**D.O.F. 3**	**D.O.F. 4**	**D.O.F. 5**	**D.O.F. 6**
Direction	X	Y	Z	Rx	Ry	Rz
Translation/Rotation	U1	U2	U3	UR1	UR2	UR3

ISSN 2176-5480

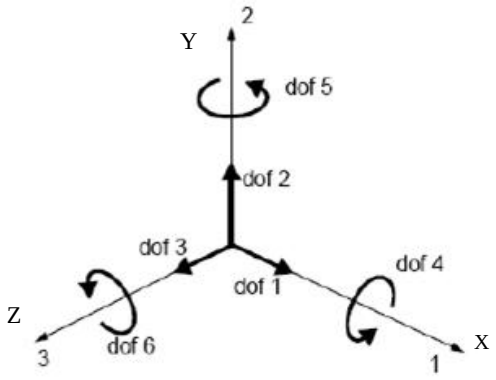

Figure 7. Degree of Freedom Convention - *ABAQUS* (2010)

At the top and bottom edge were applied different constraints, such as those shown in Table 4. The prescribed displacement is identified as *BC-3* and is a displacement of 1mm, applied to the top edge compressing the plate.

Table 4. Description of Analyzed Models (BC – Boundary Condition)

Model	**# Boundary Condition**	**D.O.F. Bottom Edge**	**# Boundary Condition**	**D.O.F. Top Edge**	**# Boundary Condition**	**Prescribed Displacement in Y**
Model 1	BC-1	123	BC-2	356	BC-3	-1 mm
Model 2	BC-5 BC-7	1* 23	BC-2 BC-4	356 1**	BC-3	-1 mm
Model 3	BC-1	123	BC-2 BC-6	356 1***	BC-3	-1 mm

* Only 1 central node constrained on bottom edge
** Only 1 central node constrained on top edge
*** All top nodes constrained

Figure 8 illustrates the boundary conditions on top and bottom edges (*BC-Top* and *BC-Bottom*), as well as the prescribed displacement applied on top edge.

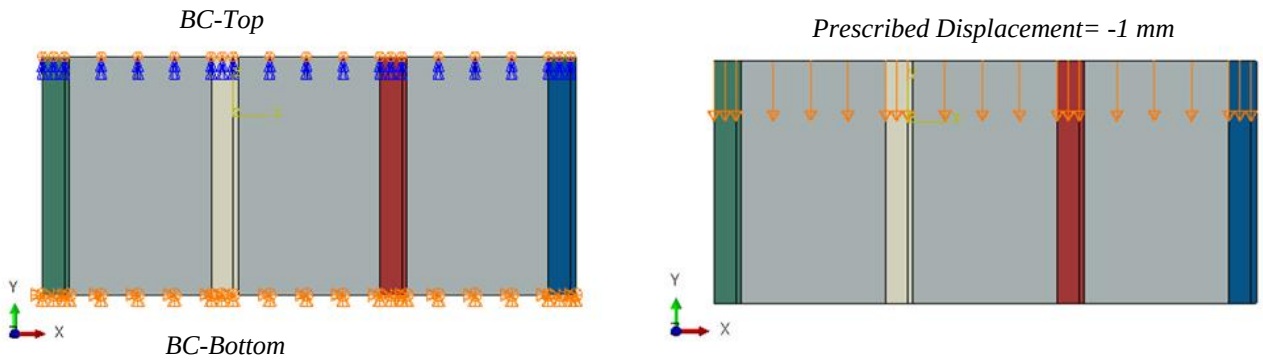

Figure 8. Models Configuration (top and bottom edge constrained, lateral edge free)

4. MODEL ANALYSIS

The models were analyzed for buckling and post-buckling behavior. The analysis of buckling is considered in the linear regime of the material. For the post-buckling behavior is necessary to take into account the plasticity of the material (aluminum 2024-T3 and 7075-T62) and the geometric nonlinearities. By static model analysis is possible to determine the total load applied to the model making the sum of the reaction forces (RF_2) in the direction Y. Performing linear perturbation analysis is obtained the buckling eigenvalue to calculate the buckling load P_{cr} which is obtained by multiplying the first eigenvalue (λ) to the total load applied (P_T).

ISSN 2176-5480

5. RESULTS AND DISCUSSION

The following are the results obtained by the software ABAQUS. The results are presented in the order: Model 1, Model 2 and Model 3.

For this analysis there are variations of boundary conditions and application of -1mm displacement at the top edge of the plate. It was carried out the Linear Buckling Solution. Figure 9 shows the buckling mode and the first eigenvalue for each model. Table 5 shows the summary results for each model.

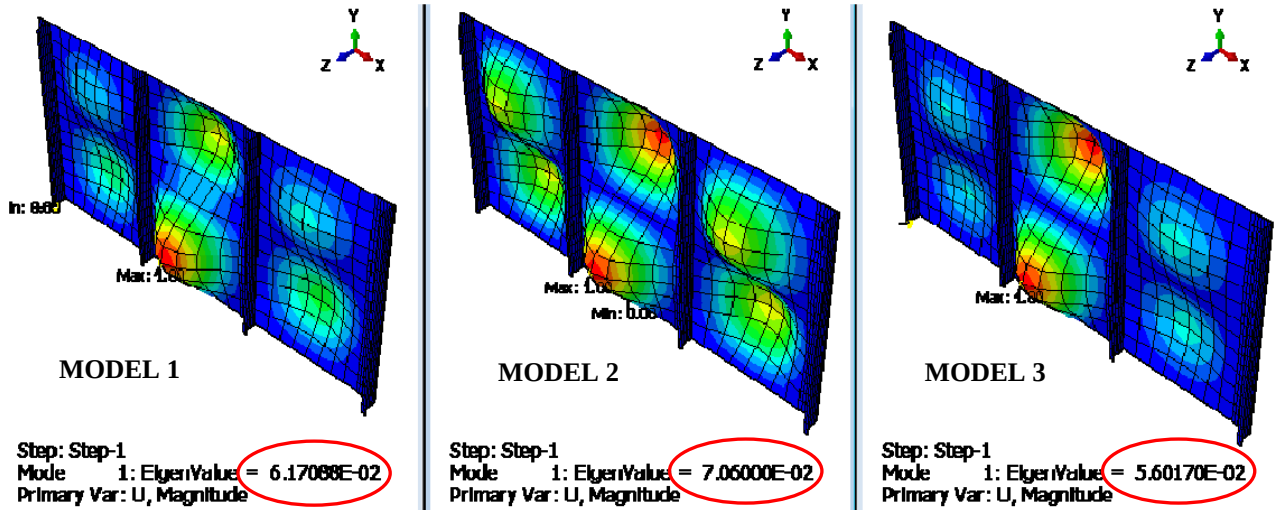

Figure 9. Linear Buckling Analysis – 1st eigenvalue (1st mode)

Table 5. Buckling Analysis Results

Model	P_T (kN)	1st eigenvalue	P_{cr} (FEM) (kN)	F_{cr} (MEF) (MPa)	P_{cr} (Theoretical) (kN)	Var (*)
1	255.66	6.17E-02	15.77	20.8	14.12	11.75
2	248.82	7.06E-02	17.57	23.1	14.12	24.44
3	262.32	5.60E-02	14.69	19.3	14.12	4.07

(*)Var= 100* ($P_{cr, FEM}$ - $P_{cr, Theoretical}$)/ $P_{cr, Theoretical}$ (%)

Using the same models, but changing the type of solution to Static General, in order to perform the post buckling analysis, it was taking into account plasticity of material and geometric nonlinearities. Initial imperfections have not been considered to the models.

Figure 10 presents the Von Mises stress for the skin. It is possible that observer for Model 1, that there is localized stress concentration in the region of stringers, precisely where there is a degradation and initial failure of the adhesive. However for the stringers shown in Figure 11 that after 100% of the load applied (when the total displacement of -1 mm was used), there is no stringer yielding, the Von Mises stress didn't reach material yielding (490 MPa).

Figure 12 illustrates the behavior of degradation and failure of the adhesive at stringer-2. It is observed along the degradation criterion curve (*CSQUADSC*) that the adhesive deteriorates when the criterion is satisfied, ie where *CSQUADSC* is equal to 1, it happens when 63.65% of load is applied. In this period, the adhesive has not been failed yet. However, after the occurrence of the degradation, the adhesive begins to fail at the same time of total degradation (again 63.65% of load applied) and the fail completely when *CSDMG* is satisfied, in other words, equal to 1 in 71.60% of applied load. This analysis shows that, the adhesive will fail before total load applied (100% of prescribed displacement = - 1mm). Despite the adhesive failure at stringer-2, the panel can still withstand loads through the remaining stringers.

ISSN 2176-5480

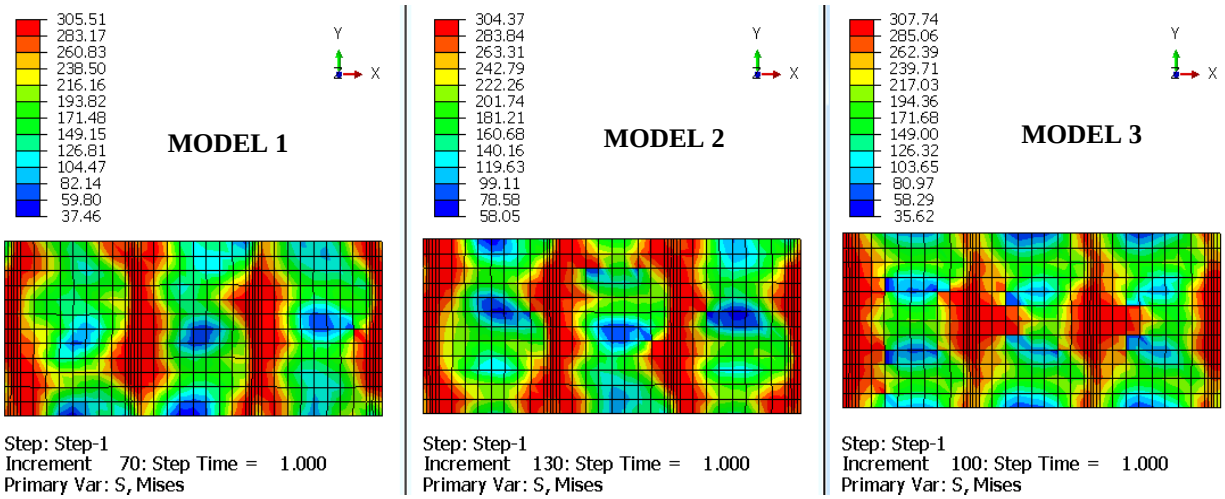

Figure 10. Von Mises Stress – Skin

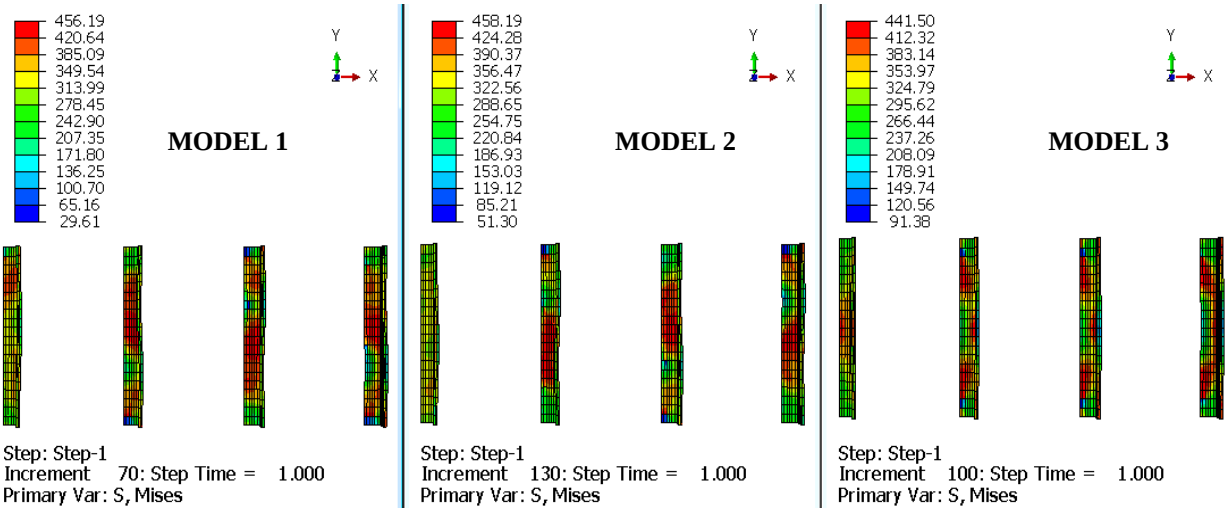

Figure 11. Von Mises Stress – Stringers

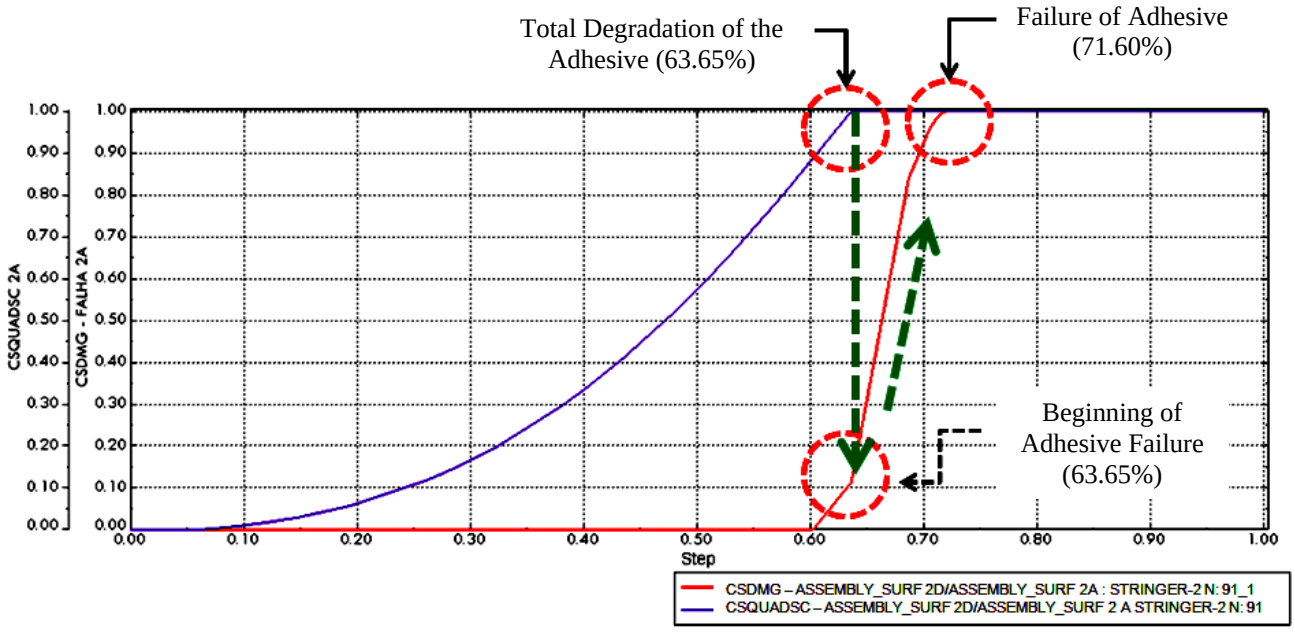

Figure 12. Degradation and Adhesive Failure Process

ISSN 2176-5480

Figure 13 and Figure 14 show typical results for all models considering the degradation and failure of the adhesive located in the stringer-2. It is noted that the adhesive in the stringer-s degrade around 63% of the applied load. The adhesive of the first stringer for all models did not degrade (*CSQUADSC* always lesser than 1) and consequently there is no failure of adhesive (*CSDMG* is always zero).

The adhesive failure for Model 1 is around 71% of the load applied. As for the Model 2, this failure load is higher, around 76%. Finally for Model 3 there is no failure of the adhesive. These behavioral differences are due to the boundary condition applied. The models are very sensitive to these variations. The following figures illustrate the degradation and failure of the adhesive according to the percentage of applied load.

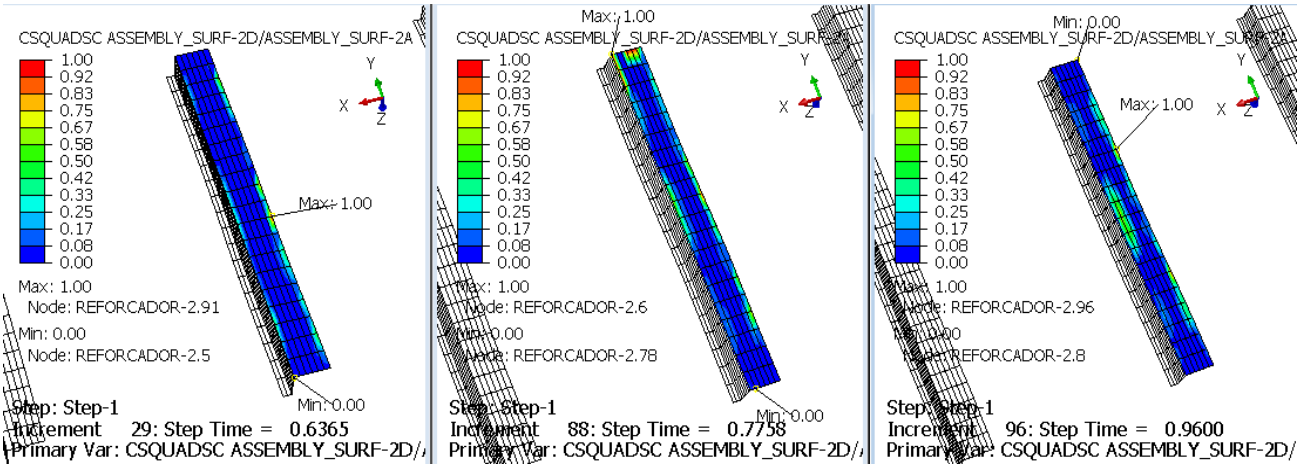

Figure 13. Degradation of Adhesive – Stringer-2

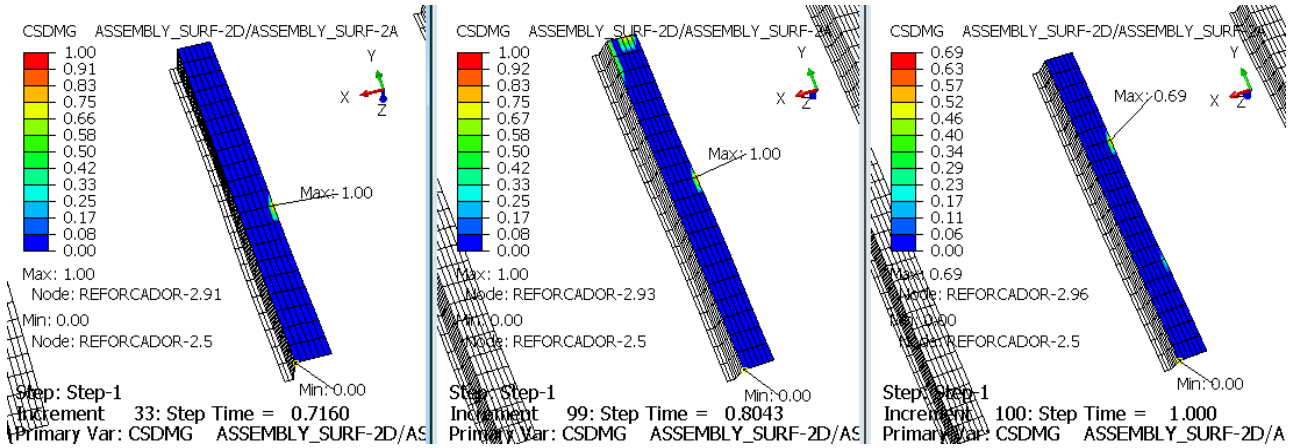

Figure 14. Failure of Adhesive – Stringer-2

5.1 Evolution Curve of the Panel

Figure 15 presents the behavior of the skin-stringer-adhesive assembly. Initially it is taken buckling results as the first point of the curve which occurs before 10% of the applied load. This phenomenon is explained due to the thin thickness of the skin. In the sequence it can be seen the behavior of the panel after the buckling. First there is the skin yielding, degradation of adhesive, adhesive failure and stringer yielding. The dashed lines indicate load prediction for the failure of the skin, the stringer and finally the total collapse of the panel. It is noted that for Model 3 there is no adhesive failure. For Models 1 and 2, the first stringers to fail are the numbers 2 and 3. It seems that the collapse of the panel occurs approximately at 280 kN load. Skin and stringers' failure can be observed when they reach the F_{TU} (material allowable). It's important to notice that all the results shown in this paper can be seen through the Finite Element Model (FEM). However, skin and stringers' failure must be better confirmed with further studies. Nevertheless, the whole relevance of this study should be confirmed in future tests to confirm the theoretical values presented here.

ISSN 2176-5480

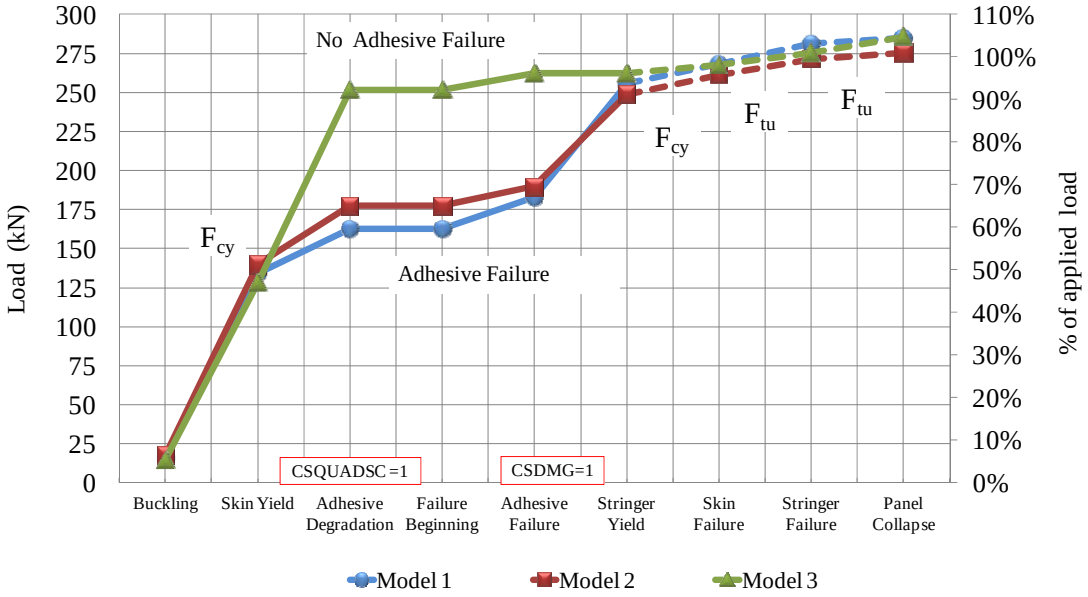

Figure 15. Final Results – Panel Evolution

6. CONCLUSIONS

The proposed model for the analysis of a panel with bonded stringers subjected to compressive load was able to produce good results regarding prediction of buckling load. It was possible to access the values of degradation and failure in the adhesive layer. The datum found indicate that the adhesive resists to buckling load, but would most likely fail before the full yielding of the panel. The models are very sensitive to the boundary conditions, however observing the numerical values of the linear buckling load it is noted that the Models 1 and 2, led to similar values. Additionally, they correlate better with the theoretical result. It can be seen by non-linear analysis, that the buckling load obtained from the models approach the linear analysis. Buckling occurs before 10% of the applied load for all models (in the linear phase of the material). With respect to the beginning of the adhesive's disbonding, it is noted that Model 1 is the most critical one, but about the failure, Model 1 and 2, show close load values. Model 3, degrades but not enough to fail when final load is applied. The adhesive of stringer 2 and 3 of Model 1 was the most critical one, followed by Model 2. The total failure of the adhesive in Model 1 occurs at 72% after all the stringers' adhesive has failed, with the exception of the adhesive on stringer-1. For model 2, the value of the complete failure of the adhesive occurs when 76% of the load was applied. All in all, the skin yielding happens before the adhesive degradation and failure. Therefore, it can be observed that the stringers' yielding take longer to fail and have to go through all adhesive steps (degradation and failure). After the failure of all bonded stringers, the skin / stringers still have resistance to withstand load, but the collapse will occur after rupture of the skin and stringer as shown in the graph.

7. REFERENCES

Abaqus, 2010. *User's Manual*. Version 6.10. HKS Inc. USA.

Bruhn, E.F., 1973. *Analysis and Design of Flight Vehicle Structures*. Purdue University, Indiana.

Castelani, T. 2012. *Otimização e dimensionamento de perfis formados a frio pelo método de resistência direta*. 2012. Msc thesis, Universidade Federal do Rio Grande do Sul, Porto Alegre.

Dean, G.; Crocker, L. 2001. Measurement good practice guide no, 48: the use of finite element methods for design with adhesive. Teddington: National Physical Laboratory.

Megson, T.H.G. *1999. Aircraft Structures for Engineering Students*. 3a edicao. Great Britain: by MPG Books Ltd. Bodmin. Cornwall.

Paulino, L. T. 2009. *Estudo da Resistência a Flambagem em Perfis Formados a Frio*. Monografy. Universidade federal do Rio Grande do Sul. Porto Alegre.

FAA/DOD/NASA-MMPDS-03. 2006. *Metallic Material Properties Development and Standardization.U.S.* Department of Transportation Federal Aviation Administration. Handbook.

Rizzi, P. 2007. *Estabilidade de Estruturas Aeronáuticas*. Instituto Tecnológico de Aeronáutica. São José dos Campos.

ISSN 2176-5480

Gavazzi, A. 2012. “Delamination Analysis Through Abaqus Cohesive Finite Elements”. In: *17th Composite Durability Worksho.*. São José Dos Campos. Brasil.

Linde, P.; Pleitner. J.; Boer, H. de.; Carmone, C. 2004. Modelling and Simulation of Fibre Metal Laminates. In: *ABAQUS Users’ Conference*. *23 out. 2012.* <http://www.simulia.com/download/solutions/aerospace_cust%20references/Composites_Advanced_AUC04_ALE_Airbus.pdf.>

Ramamurthi. M.. KIM.Y.S 2012. “Delamination Characterization of Bonded Interface Using Surface Based Cohesive Model: Suplemental Proceedings: Volume 1: In: *The Minerals. Metals & Materials Society Materials Processing and Interfaces TMS.*

Reddy Racha. S.K. 2008. An abstract of a thesis damage characterization of four wrought aluminum alloys. Msc thesis. Faculdade de Tecnologia. Tennessee.

8. RESPONSIBILITY NOTICE

The author(s) is (are) the only responsible for the printed material included in this paper.